Thin Solid Films 518 (2010) 3813–3818

Contents lists available at ScienceDirect

Thin Solid Films

journal homepage: www.elsevier.com/locate/tsf

Surface mound formation during epitaxial growth of CrN(001)

X.Y. Zhang, D. Gall *

Department of Materials Science and Engineering, Rensselaer Polytechnic Institute, Troy, NY 12180, USA

ARTICLE INFO

Article history:
Received 26 October 2009
Received in revised form 6 December 2009
Accepted 9 December 2009
Available online 16 December 2009

Keywords:
Chromium nitride
Surface morphology
Hard coating
Scanning tunneling microscopy

ABSTRACT

Single crystal CrN(001) layers, 10 to 160 nm thick, were grown on MgO(001) by reactive magnetron sputtering at growth temperatures $T_s = 600$ and 800 °C. *In situ* scanning tunneling microscopy shows that all layer surfaces exhibit mounds with atomically smooth terraces that are separated by monolayer-high step edges aligned along (110) directions, indicating N-rich surface islands. For $T_s = 600$ °C, the root mean square surface roughness σ initially increases sharply from 0.7 ± 0.2 for a thickness $t = 10$ nm to 2.4 ± 0.5 nm for $t = 20$ nm, but then remains constant at $\sigma = 2.43 \pm 0.13$ nm for $t = 40$, 80 and 160 nm. The mounds exhibit square shapes with edges along (110) directions for $t \leq 40$ nm, but develop dendritic shapes at $t = 80$ nm which revert back to squares at $t = 160$ nm. This is associated with a lateral mound growth that is followed by coarsening, yielding a decrease in the mound density from 5700 to 700 μm^{-2} and an initial increase in the lateral coherence length ξ from 7.2 ± 0.6 to 16.3 ± 0.8 to 24 ± 3 nm for $t = 10$, 20, and 40 nm, respectively, followed by a drop in ξ to 22 ± 2 and 16 ± 2 nm for $t = 80$ and 160 nm, respectively. Growth at $T_s = 800$ °C results in opposite trends: σ and ξ decrease by a factor of 2, from 2.0 ± 0.4 and 20 ± 4 nm for $t = 10$ nm to 0.92 ± 0.07 and 10.3 ± 0.4 nm for $t = 20$ nm, respectively, while the mound density remains approximately constant at 900 μm^{-2}. This unexpected trend is associated with mounds that elongate and join along (100) directions, yielding long chains of interconnected square mounds for $t = 40$ nm. However, coalescence during continued growth to $t = 160$ nm reduces the mound density to 100 μm^{-2} and increases σ and ξ to 2.5 ± 0.1 and 40 ± 2 nm, respectively.

1. Introduction

Transition-metal nitrides are widely used as protective coating materials, as they exhibit remarkable physical properties including high hardness and mechanical strength, chemical inertness, and high-temperature stability. CrN has gained considerable interest in particular due to its superior high-temperature oxidation resistance [1–3], which is higher than that for TiN, the most common nitride hard coating. CrN shows high wear [4,5] and corrosion resistance [6], improves system adherence as an interfacial layer between diamond films and steel [7], and offers potential for use in phase-shift masks for photolithography [8], in etch resistant hardmasks for X-ray absorber patterning [9] as hard matrices in self-lubricating coatings [10–12], as thermoelectric materials [13] and as catalyst support for fuel cells [14]. CrN also exhibits unique electronic properties which are still not well understood, with reported room temperature resistivity values ranging from 304 to 2.1×10^7 μΩ cm [15–22], a temperature coefficient for resistivity which is positive [20,21] or negative [15,20], a phase transition to an orthorhombic structure when cooling below 273–286 K which is associated with antiferromagnetic ordering [23–25], and a possible band gap of 0.07–0.1 eV [15,26,27]. In order to exploit these unique electronic properties of CrN and to improve mechanical and thermal stability for above applications, it is important to develop a detailed understanding of the kinetic pathways during growth that control the microstructural evolution, in particular the grain size and texture, porosity, composition, and surface morphology. Previous studies have shown that ion irradiation and partial gas pressure strongly affect both texture [28] and surface morphology [29,30], atomic shadowing causes exacerbated surface roughening [31] and leads to the development of straight [29] and tilted pores [32], and epitaxial growth results in smooth surfaces [33] with 1–5 nm wide atomically flat terraces [26]. We build on these reported results and use the growth of epitaxial CrN(001) as a model system to study the CrN microstructural evolution.

In this article, we focus in particular on the surface morphological evolution of single crystal CrN(001) grown on MgO(001) by ultrahigh vacuum (UHV) reactive magnetron sputter deposition at growth temperatures $T_s = 600$ and 800 °C, and with increasing layer thickness $t = 10$–160 nm. The CrN(001) surfaces exhibit (110) step edges and 1–10 nm wide atomically smooth terraces, as observed by *in situ* scanning tunneling microscopy (STM). Growth at 600 °C leads to surface mounds which have square shapes and edges along (110) directions for $t \leq 40$ nm, develop dendritic shapes for $t = 80$ nm, and join during continued growth to revert back to squares at $t = 160$ nm. In contrast, at $T_s = 800$ °C mounds elongate and join along (100) directions with curved edges, yielding long chains of interconnected square mounds for $t \leq 40$ nm, which are subsequently overgrown by rapidly growing mounds with (110) edges. The dramatic difference in

---

* Corresponding author.
E-mail address: galld@rpi.edu (D. Gall).

0040-6090/$ – see front matter © 2009 Elsevier B.V. All rights reserved.
doi:10.1016/j.tsf.2009.12.085

mound development for $T_s = 600$ and 800 °C is attributed to the increasing adatom diffusion length at increasing growth temperature.

2. Experimental procedure

All CrN layers were grown in a load-locked UHV dc magnetron sputtering system with a base pressure of 1.3×10^{-7} Pa (1×10^{-9} Torr), achieved by a 520 l s^{-1} turbomolecular pump. The substrates were single-side polished $10 \times 10 \times 0.5$ mm^3 MgO(001) wafers, cleaned with successive ultrasonic baths of trichloroethylene, acetone, and isopropanol, rinsed with de-ionized water, and then blown dry with dry nitrogen [34]. A conductive contact was painted from the front to the back of the insulating substrates, using colloidal graphite, in order to ensure electric contact during STM analyses. The samples were then secured to a stainless steel backing plate by mechanical clamping and by silver paint, which was cured on a hot plate at 150 °C for 10 min. The backing plates were mounted to a molybdenum holder and inserted into the load-lock system for transfer to the growth chamber where the substrates were degassed for 1 h at 800 °C. The substrate temperature T_s was measured by a *C*-type thermocouple located within the sample stage and confirmed by optical pyrometry. N_2 (99.999% pure) was further purified through a Micro Torr purifier and introduced into the deposition chamber to provide a constant pressure of 0.40 Pa (3 mTorr), as measured with a capacitance manometer. A water-cooled 5-cm-diameter 99.95% pure Cr target was positioned at 10.5 cm from the substrate at an angle of 45° with respect to the substrate surface, which was continuously rotated to maximize layer uniformity. Immediately before deposition, the target was sputter cleaned for 5 min with a protective shield covering the substrate. Layers were grown at a constant power of 350 W, resulting in a growth rate of 25 nm/min, as determined using Rutherford Backscattering Spectroscopy (RBS) on calibration samples.

After deposition, the samples were allowed to cool in vacuum to <90 °C prior to vacuum-transfer to the analysis chamber with a base pressure $< 1.3 \times 10^{-6}$ Pa ($< 1 \times 10^{-8}$ Torr), maintained with a 300 l s^{-1} ion pump. The surface morphologies were characterized using an Omicron *in situ* STM, with a commercially prepared tungsten tip, a bias voltage of 0.5 V, and a constant tunneling current of 0.5 nA. The scanning direction was for all samples parallel to the substrate edge. Therefore, for all micrographs in this manuscript, the scanning direction is horizontal and corresponds to the [100] crystal orientation of the MgO(001) substrates, while the vertical direction in the micrographs is parallel to [010]. Quantitative surface morphological analyses were performed by independently determining height–height correlation functions for 3–6 distinct STM micrographs for each surface, using the GWYDDION software package. This provides values for the average correlation length ξ and the root mean square (rms) surface roughness σ. The latter values are in good agreement with the values determined using the Omicron SCALA® software. The uncertainties in the parameters ξ and σ are estimated by independently analyzing a set consisting of a minimum of three micrographs obtained from different regions of the same sample surface.

3. Results and discussion

All CrN layers are complete single crystals, with a cube-on-cube epitaxial relationship with the substrate, $(001)_{CrN} \| (001)_{MgO}$ and $[001]_{CrN} \| [001]_{MgO}$, as determined by X-ray diffraction ω–2θ and pole figure analyses.

Fig. 1 shows an exemplary *in situ* scanning tunneling micrograph from a 100×100 nm^2 surface area of a 40-nm-thick CrN(001)/MgO (001) layer grown at $T_s = 800$ °C. It reveals atomically smooth terraces that are separated by steps with a measured average height of 2.1 Å. This value is close to 2.07 Å, the interplanar spacing along (100) of cubic rock-salt structure CrN with a reported lattice constant of 4.14 Å [26], indicating that the observed steps have a height of one monolayer. The terraces have a width of 1–10 nm and form 20–40 nm wide mounds that are 10–15 monolayers high, corresponding to a height-to-width aspect ratio of 0.10 ± 0.03. The dark areas in the micrograph are from relatively narrow trenches between surface mounds, with steep slopes so that single-atom-high steps cannot be resolved with the employed STM imaging conditions and tip radius. The surface steps in Fig. 1 show a strong tendency to align along crystalline (110) directions. This step orientation along (110) is observed for all thicknesses $t = 10$–160 nm and both growth temperatures $T_s = 600$ and 800 °C, and indicates non-stoichiometric surface islands, as discussed in the following paragraph.

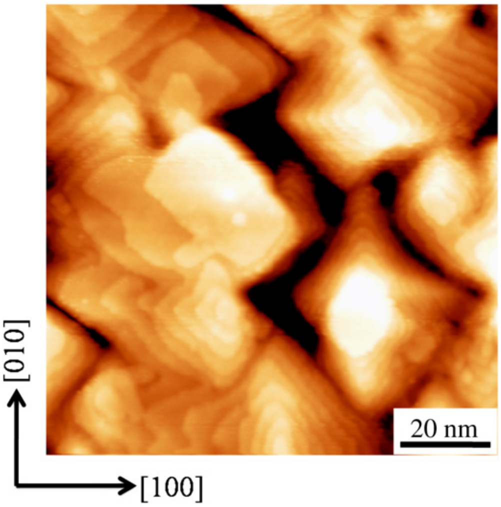

Fig. 1. *In situ* scanning tunneling micrograph from a 100×100 nm^2 surface area of a 40-nm-thick epitaxial CrN(001)/MgO(001) layer grown at $T_s = 800$ °C.

Previous studies on the morphology of (001) surfaces of cubic NaCl-structure TM nitrides report both (100) and (110) directions for surface steps and/or mounds: TiN(001) was found to exhibit square surface mounds with edges along (100) when sputter deposited in a pure N_2 atmosphere at 1050 °C [35], or when deposited by reactive evaporation at 750 °C [36], but has dendritic islands with fingers extending towards (110) when grown at a reduced N_2 partial pressure at 740 °C [37], and develops ridges along (110) for low N_2 flux, including for under-stoichiometric $TiN_{0.92}$ [38]. ScN(001) exhibits square islands with edges along (100) under N-rich conditions [39] but shows rounded islands and mounds for understoichiometric (i.e. Sc-rich) ScN_x [40], and also in some cases islands terminated by 8 alternating (100) and (110) step edges [41]. The few reports on CrN(001) suggest (110) step edges for vacancy islands that form during growth by molecular-beam epitaxy at 650 °C [26], but square mounds with (100) step edges for growth by magnetron sputtering at 570–700 °C in a 2.7 Pa nitrogen atmosphere [29,33]. In summary, these published results on TiN(001), ScN(001), and CrN(001) suggest that the nitrogen flow strongly affects if surface islands are terminated by (100) or (110) step edges. We attribute this to the fact that (100) step edges are stoichiometric, while (110) edges are polar, that is (110) edges are either terminated by nitrogen or metal atoms, making the surface island N- or metal-rich. Consequently, deposition conditions that lead to a high steady-state N surface coverage [42] may favor N-terminated step edges, i.e. (110)-oriented edges. Correspondingly, understoichiometric growth with metal-rich surfaces leads to metal-terminated edges which are also (110)-oriented, while growth conditions between these two extremes leads to stoichiometric (100) edges. We attribute the (110)-oriented step edges for our CrN(001) surface islands to N-termination, since for our deposition process, the N_2 flux impinging on the growing surface from the 0.40 Pa atmosphere is three orders of magnitude larger than the Cr flux, which is determined from the deposition rate.